RJC

RASĀYAN *J. Chem.*
Vol. 13 | No. 3 |1999-2009| July - September | 2020
ISSN: 0974-1496 | e-ISSN: 0976-0083 | CODEN: RJCABP
http://www.rasayanjournal.com
http://www.rasayanjournal.co.in

MORPHOLOGICAL AND CRYSTALLINE PHASE CHANGES OF $CaCO_3$ PRECIPITATES UNDER THE INFLUENCE OF MALONIC ACID

S. Muryanto[1,*], S. Sutanti[2], E. Supriyo[3] and W.A. Putranto[4]

[1]Department of Chemical Engineering, UNTAG University in Semarang, Semarang 50233, Indonesia

[2]Department of Chemical Engineering, Politeknik Katolik Mangunwijaya, Semarang 50242, Indonesia

[3]Chemical Engineering Vocational School, DIPONEGORO University, Semarang 50275, Indonesia

[4]Department of Mechanical Engineering, Politeknik Maritim Negeri Indonesia (Polimarin), Semarang 50233, Indonesia

*E-mail: stmuryanto@untagsmg.ac.id

ABSTRACT

Industrial applications of calcium carbonate ($CaCO_3$) are dictated by its crystalline properties. To a large extent, $CaCO_3$ scaling which is prevalent in industrial equipment is also governed by such properties. A thorough comprehension of the modification of $CaCO_3$ properties is thus essential. The current work describes $CaCO_3$ precipitation using the well-established drop-wise method in which the solution of Na_2CO_3 was dripped into $CaCl_2$ solution with agitation. Minute (ppm) amounts of malonic acid were added during precipitation to investigate its effects on the $CaCO_3$ crystal properties, either in the pure system or when the acid was added. Precipitates obtained were quickly filtered, centrifuged, and subsequently dried in an oven at 60°C. SEM, XRD, FTIR and DT-TGA were used to characterize the precipitates. The experiments showed that amorphous calcium carbonate initially precipitated and gradually converted into calcite via vaterite and aragonite. This study aimed to ascertain the influence of malonic acid on precipitation of $CaCO_3$ with the intention for practical applications in mitigating $CaCO_3$ scaling. The findings suggest that malonic acid was capable to induce vaterite growth in solution. In line with our hypothesis, an increase in the addition of malonic acid (ppm amounts) is accompanied by more vaterite phase alongside calcite.

Keywords: Aragonite, $CaCO_3$, Calcite, Malonic Acid, Vaterite.

INTRODUCTION

Crystalline phases and morphology of $CaCO_3$ are crucial for the industrial applications of this carbonate mineral. Further, $CaCO_3$ is one of the main components of scale which can develop in industrial equipment, particularly in the piping system and heat exchangers. Similarly, the properties of the $CaCO_3$ scale are often dictated by the phases and morphological nature of the crystals[1]. Under ambient conditions and in a pure precipitation system the crystalline carbonate mineral comprises three phases, namely vaterite, aragonite, and calcite, and two hydrous crystalline forms: $CaCO_3.H_2O$, and $CaCO_3.6H_2O$ [2,3,4,5]. Among the three anhydrous phases, calcite is thermodynamically stable at atmospheric conditions, while vaterite is the least.[6]

The growth rate of both calcite and aragonite was found to be significantly retarded by citric acid. This was reported by Westin and Rasmuson in their precipitation work on $CaCO_3$ using the well-established constant supersaturation method.[7] The supersaturation level was maintained at 4.0 and the solution pH was 8.0. The retardation was due to the complexation of the calcium ions in the solution with the carboxylic functional groups. A higher concentration of citric acid resulted in more inhibition. Due to

CrossMark

differences in the dominant crystal faces of either aragonite, vaterite, or calcite, citric acid was more efficient in inhibiting the growth of aragonite than that of calcite.

Carboxylic acids could inhibit the growth of calcite through adsorption of the functional groups of the acids onto the calcite growth sites. Such adsorption can be very effective. As reported, 0.50 ppm of fulvic acid has been shown to retard calcite growth by 47%, at a supersaturation level of 4.5. and solution pH of 8.5.[8] It was postulated that the intensity of inhibition was positively correlated with the number of the functional groups. The adsorption could either be chemical or physical and the mechanism was through linking of H^+ in the carboxylic groups and CO_3^{2-} on the surface of calcite.[9]

Growth of calcite as one of the components of scale in many industrial processes was also inhibited by carboxylic acids. Mangestiyono et al reported that both formic and oxalic acids were able to retard calcite formation by as much as 13% and 26%, respectively.[10] In their investigation, they have applied vibration during the precipitation, to mimic the real conditions in industrial processing. It was also found that under high vibration, i.e. 6.00 Hz, the weight of the calcium carbonate crystals formed, calcite included, was three times higher than that in the absence of vibration. However, the vibration prevented the agglomeration of the crystals which is beneficial for $CaCO_3$ scale development.

Tartaric, maleic and citric acids were found to lengthen induction time and modify the habit of $CaSO_4$.[11] Recently, Karaman et al reported that the precipitation of barite ($BaSO_4$) was affected by the addition of carboxylic acids, commonly recognized as green inhibitors.[12] Karaman et al were able to identify the modifying performance of these acids, on $BaSO_4$ morphology and growth rate, precipitated in a flowing system and affected by vibration. It was not yet clear, however, whether dissimilar functional groups of these acids affected the properties of the $BaSO_4$ differently.

During precipitation of $CaCO_3$ in the presence of lithium ions, nucleation and growth of both aragonite and vaterite could occur simultaneously with the change in habit of calcite. Such a mechanism was caused by these foreign metallic adsorbed onto the surface of calcite crystals and subsequently formed 2D nuclei. As reported, the epitaxy aragonite/2D-Li_2CO_3 decreased the specific surface energy of aragonite and led to the evolution of aragonite.[13]

A significant influence on crystal growth and habit would materialize only if the interaction between $CaCO_3$ crystals and carboxylic molecules was intense.[14] Additionally, the size of the molecules also decisively affects such properties. Such findings suggest that the influence of poly-(aspartic acid) (PAA) on habit and morphology is greater than that of succinic acid. PAA lead to granules or nanostructured precipitates, while in the presence of succinic acid the morphology remained essentially the same.

Malonic acid is a white crystalline powder, a di-carboxylic acid, and also known as propanedioic acid. Its chemical formula is $C_3H_4O_4$ or $COOHCH_2COOH$. Malonic acid is a basic component in various industries: petrochemical, pharmaceutical, cosmetics, specialty chemicals, food and drugs and so on. [15] This acid occurs naturally in air due to photocatalytic reactions of cyclic olefins and other hydrocarbons emitted from engines, wood fires, as well as cigarettes. Malonic acid also occurs in various plants, especially in fruits and grains. Physically, malonic acid is very soluble in water; hence waste streams from the previously cited industries may contain malonic acid. As stated previously in the Introduction, various carboxylic acids are effective in modifying the precipitation behavior and properties of inorganic minerals, including $CaCO_3$. However, malonic acid has not yet been tested as such, especially to investigate $CaCO_3$ scale formation and inhibition. This paper describes the results of a study to ascertain the effects of malonic acid on precipitation of $CaCO_3$ with the intention for practical applications in mitigating $CaCO_3$ scaling.[10]

EXPERIMENTAL

Material and Methods

The precipitation was carried out in a batch precipitation mode using 0.5 M $CaCl_2$ and 0.5 M Na_2CO_3 solutions, following the reaction as follows:

$$CaCl_2 + Na_2CO_3 \rightarrow CaCO_3 + 2\ NaCl$$

Malonic acid [$CH_2(COOH)_2$], in the form of a weak solution, was added into the precipitating carbonate solution in varied ppm quantities, i.e. from 0.00 ppm (pure system) to 20.00 ppm.

In a typical synthesis, the precipitation run was carried out as follows. The solutions of $CaCl_2$ (50 mM, 50 mL) and Na_2CO_3 (50 mM, 50 mL) were quickly mixed in a 200-mL beaker with rigorous stirring for 30

seconds. Then the beakers were sealed and left to stay unmoved at ambient temperature. As arranged for the experimental design, the beakers were separately decanted after a pre-determined period: 5, 10, 20, and 30 mins, and then at a prolonged period of 1, 2, 6, and 48 h, respectively. Similar experiments were conducted with the addition of a malonic acid solution, where the acid was firstly added into the calcium chloride solution. The precipitates were rinsed thoroughly using distilled water and subsequently dried in a vacuum oven at 60ºC overnight. The dried precipitates were stored in vials for subsequent analysis.

Characterization

The morphology of the crystals obtained was characterized by scanning electron microscopy (SEM) at 30 kV accelerating voltage (FEI–Inspect-S-50). For the SEM analysis, the specimen was fixed on top of glass slides and then sputtered with Au.

The precipitates were also analyzed through XRD for crystalline phase identification (Philips 1830/40) with scan parameters: 5-85º 2θ, 0.020 step size, with an integration time of 15 sec/step. Radiation using Cu-Kα (λ = 1.5406 Å, 40 kV, 30 mA) was employed. The identification was done through a PC-based program of Philips X'Pert Plus. The positions and heights of the peaks were examined against the data of the standard spectrum for $CaCO_3$ (JCPDS-47-1743).

To identify that the functional groups of the malonic acid involved in the precipitation process, an FTIR analysis was conducted (Shimadzu–IR-Prestige-21). The pulverized samples were dispersed in KBr pellets. The wavenumber was fixed from 400 to 4000 $cm^{-1}$and 40 scans were recorded. Happ-Genzel appodization was employed.

To determine the thermal properties, i.e. changes of mass as a function of temperature and energetic effects, a TG-DTA analysis was performed [LINSEIS STA Platinum Series].

RESULTS AND DISCUSSION

SEM-EDX Analysis

For all experiments, the SEM micrographs show that the amount of malonic acid added, as well as the precipitation times significantly affected the morphology.

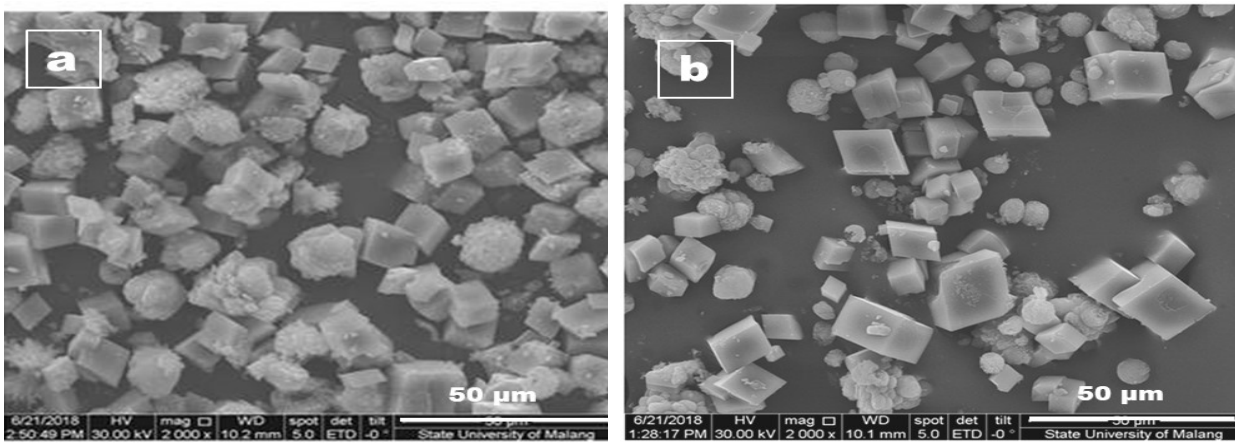

Fig.-1: SEM Graph of $CaCO_3$ Crystals in a Pure System after 4 min (a); SEM Graph of $CaCO_3$ with 20 ppm Malonic Acid after 4 min (b)

Precipitates formed in a pure system without malonic acid show the presence of all three crystalline phases in approximately similar amounts (Fig.-1a). On the contrary, the calcite phase (the cubes with sharp edges) is dominant under 20.00 ppm of malonic acid (Fig.-1b). Additionally, the two pictures reveal that the size of the phases other than calcite (irregular flat spheres) was smaller compared with those when additives were absent (Fig.-1a). It was postulated that the malonic acid functional groups may have suppressed the nucleation or retarded the growth of vaterite and aragonite. Such suppression and retardation can be due to the complexation of Ca^{2+} with functional groups of malonic acid, hence reducing the amount of Ca^{2+} required for nucleation and growth.

The change in morphology and polymorphism of $CaCO_3$ is also dependent on precipitation time.[16] Comparison of longer precipitation times both without (Fig.-2a) and with the addition of malonic acid (Fig.-2b) reveals that malonic acid has interfered with nucleation and growth as stated previously. Complexation of carboxylic functional groups with Ca ions reduces the saturation levels for the formation of $CaCO_3$.[16] This may explain the prolongation of the lifetime of the unstable phases: either vaterite or aragonite, as evident in Fig.-2b, to achieve the final and stable phase of calcite. A much shorter precipitation time, six hours compared to 48 hours, and with no additive, has resulted in the attainment of the stable phase: calcite (Fig.-2a). That the complexation of Ca-malonic acid took place was also confirmed by the FTIR spectra as discussed later in this paper (Fig.-9).

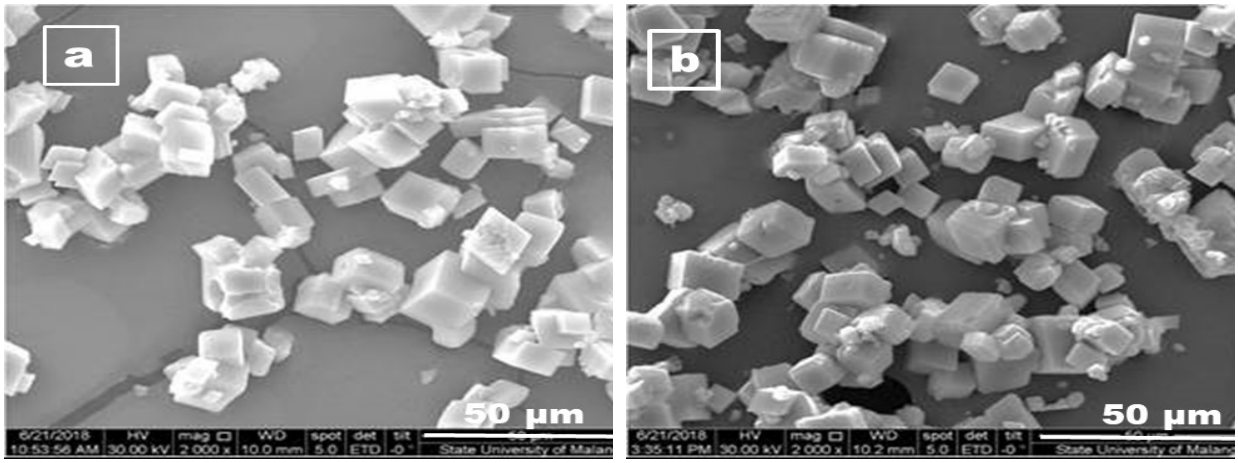

Fig.-2: SEM of $CaCO_3$ Crystals in a Pure System after six h (a); with 20 ppm Malonic Acid after 48 h (b).

Close up view of several SEM pictures, in the order of increasing precipitation times, were taken to elucidate the morphological change. This is discussed in the following (Figs.-3 to 6).

In a pure system, the edges of calcite are sharp and straight indicating a faster surface growth (Fig.-3). Additionally, both the aragonite (rosette-like) and vaterite (irregular spheres) phases seem to grow profusely. Under 20.00 ppm malonic acid (Fig.-3b), however, the calcite edges become rounded, and in certain spots, hollow and irregular surfaces appear. Furthermore, the presence of other phases: aragonite and vaterite, is less evident. As proposed by Leng et al, the morphology of calcium carbonate under the influence of carboxylic acids may demonstrate such surface imperfections due to Ostwald ripening.[16]

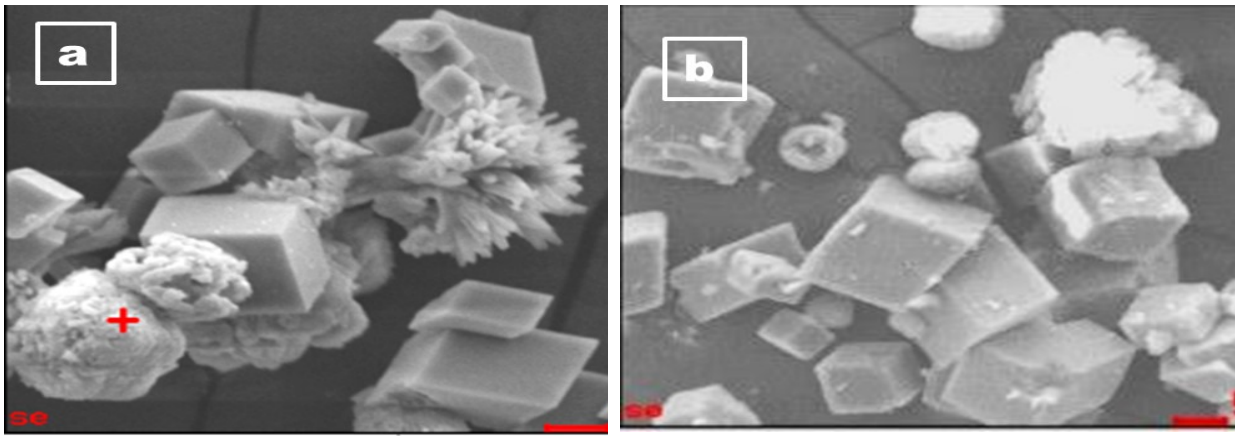

Fig.-3: SEM View of Precipitates: 4 min in a Pure System (a); 4 min with 20.00 ppm Malonic Acid (b).

A longer precipitation time of 30 min, both for pure and with malonic acid addition seems to affect the formation of aragonite. The aragonite phase grew in a pure system is morphologically perfect; whereas in the malonic acid environment, this phase seems to disappear. It was postulated that the malonic molecules were adsorbed on the nuclei surfaces and thus hindering the growth.

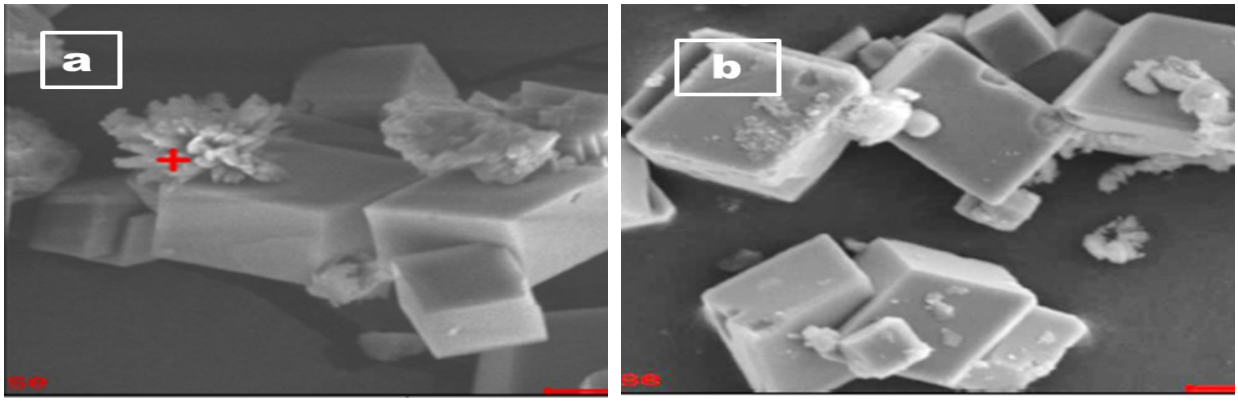

Fig.-4: SEM View of Precipitates: 30 min in a Pure System (a); 30 min with 20.00 ppm Malonic Acid (b)

Comparison between one hour of precipitation in a pure system (Fig.-5a) and with 20.00 ppm malonic acid (Fig.-5b) reveals that malonic acid has produced rounding of the edges of the rhombohedral calcite. This can be due to adsorption of malonic acid onto the surface of the crystals and prevent the oncoming of crystal units attaching to the surface or the edges of the crystals. Secondly, longer precipitation may have triggered the process of Ostwald ripening through re-crystallization.

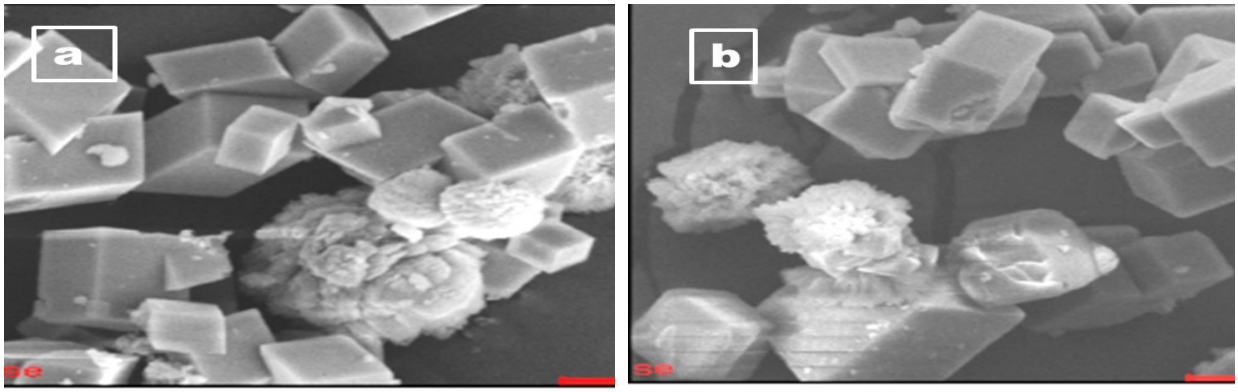

Fig.-5: SEM View of Precipitates: 60 min in a Pure System (a); 60 min with 20.00 ppm Malonic Acid (b).

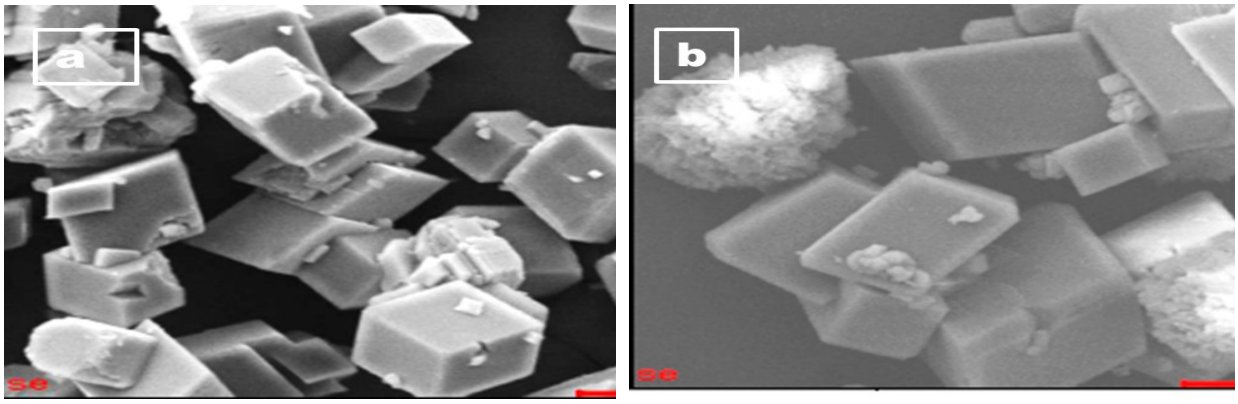

Fig.-6: SEM View of Precipitates:6 hours in a Pure System (a); 6 hours with 20.00 ppm Malonic Acid (b).

In a pure system, the edges of the calcite are still sharp (Fig.-6a), while precipitation with 20 ppm malonic shows rounding of the calcite edges (Fig.-6b). Additionally, the pure system may have enhanced the transformation of the unstable phases (both vaterite and aragonite) into the stable crystalline phase of calcite. As compared, the vaterite phase is still dominant in the presence of malonic acid (Fig.-6b)

The effect of the functional group of malonic acid differs on vaterite, aragonite, and calcite. Comparing the seeded and unseeded precipitations of $CaCO_3$ under the influence of alginate oligomers, Olderøy et al concluded that the oligomers affected the growth rate of both vaterite and aragonite, but did not affect the growth of calcite except the [104 faces].[17] Such a difference in mechanism has been identified earlier on precipitation of $CaCO_3$ with lysozyme addition, in which the calcite phase was not affected either.[18] It can be deduced, therefore, that the dissimilar crystal structure among vaterite aragonite and calcite, may cause the functional group of malonic acid to react differently with calcium ions.

X-Ray Diffraction

The XRD spectra show that the precipitates are $CaCO_3$ in its three crystalline phases: vaterite (V), aragonite (A), and calcite (C) (Fig.-7).

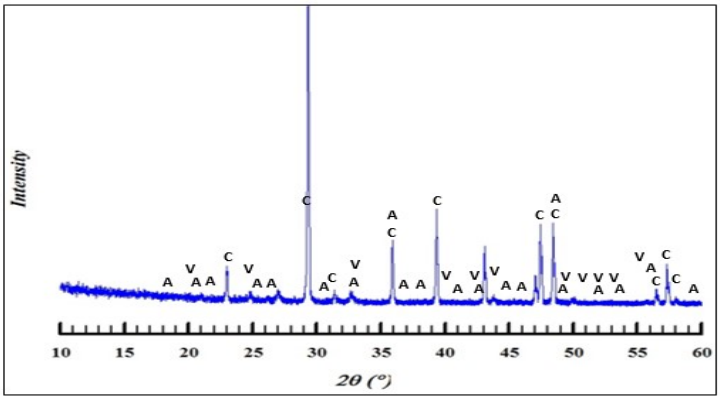

Fig.-7: Sample of the XRD Spectra Confirming the Crystalline Phases of $CaCO_3$.

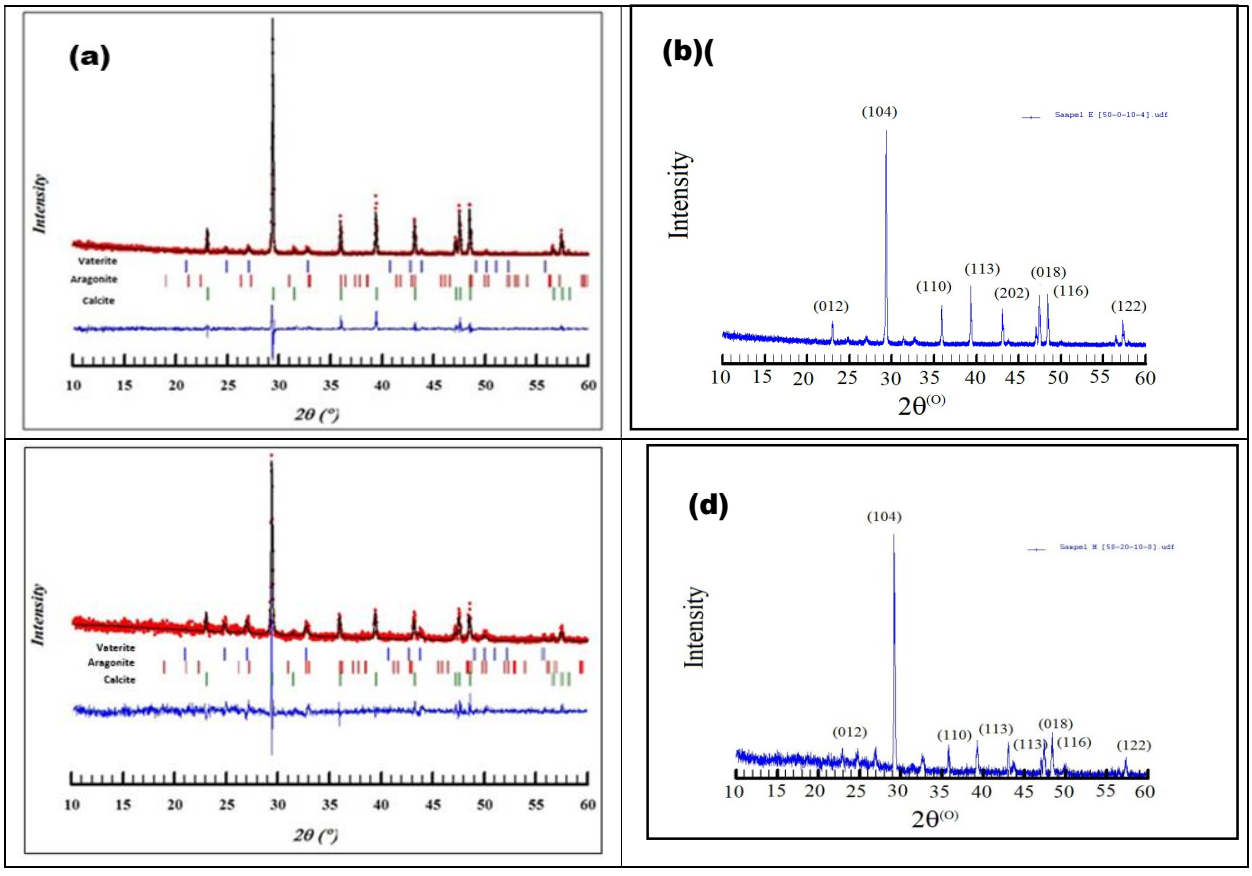

Fig.-8: XRD of $CaCO_3$ precipitated after 4 min: without Malonic Acid(a and b); with 20 ppm Malonic Acid(c and d)

The XRD spectra show the difference in the amount of the crystalline phases present (Fig.-8). In the pure system, the percentage of the three polymorphs is: vaterite=14.59%, aragonite=1.72%, and calcite=83.69%, respectively (Rietveld refinement calculation sheet not shown). In contrast, under the influence of 20.00 ppm malonic acid, the corresponding values are: 48.10%, 1.00%, and 50.90%, respectively. These data indicate the retarding effect of malonic acid on the transformation toward the stable phase, i.e calcite. The ppm amounts of malonic acid under the current experimental conditions have been able to retard the progress toward the stable phase by as much as 32.79%.

FTIR

The FTIR spectra are depicted in the following figure (Fig.-9). The spectra show sharp bands between 700 and 900 cm^{-1} and wide stretching band around 1450 cm^{-1}, confirming that the precipitates were carbonate minerals (Fig.-9)[19]. The sharp peak appears at 417 cm^{-1} can be assigned to Ca-O bond.[20] The two very sharp peaks of 712 cm^{-1} and 876 cm^{-1} correspond to in-plane and out-of-plane bending vibrations of carbonates, respectively.[16] These two peaks are characteristics of calcite. Further, the two peaks appearing at 745 and 1084 cm^{-1}, respectively, are indicative of vaterite; while that at 1088 cm^{-1} is the symmetric stretching mode (v1) of aragonite.[20] The two sharp peaks at the far left, i.e. 2509 and 2511 cm^{-1} reveal the presence of calcite.[21]

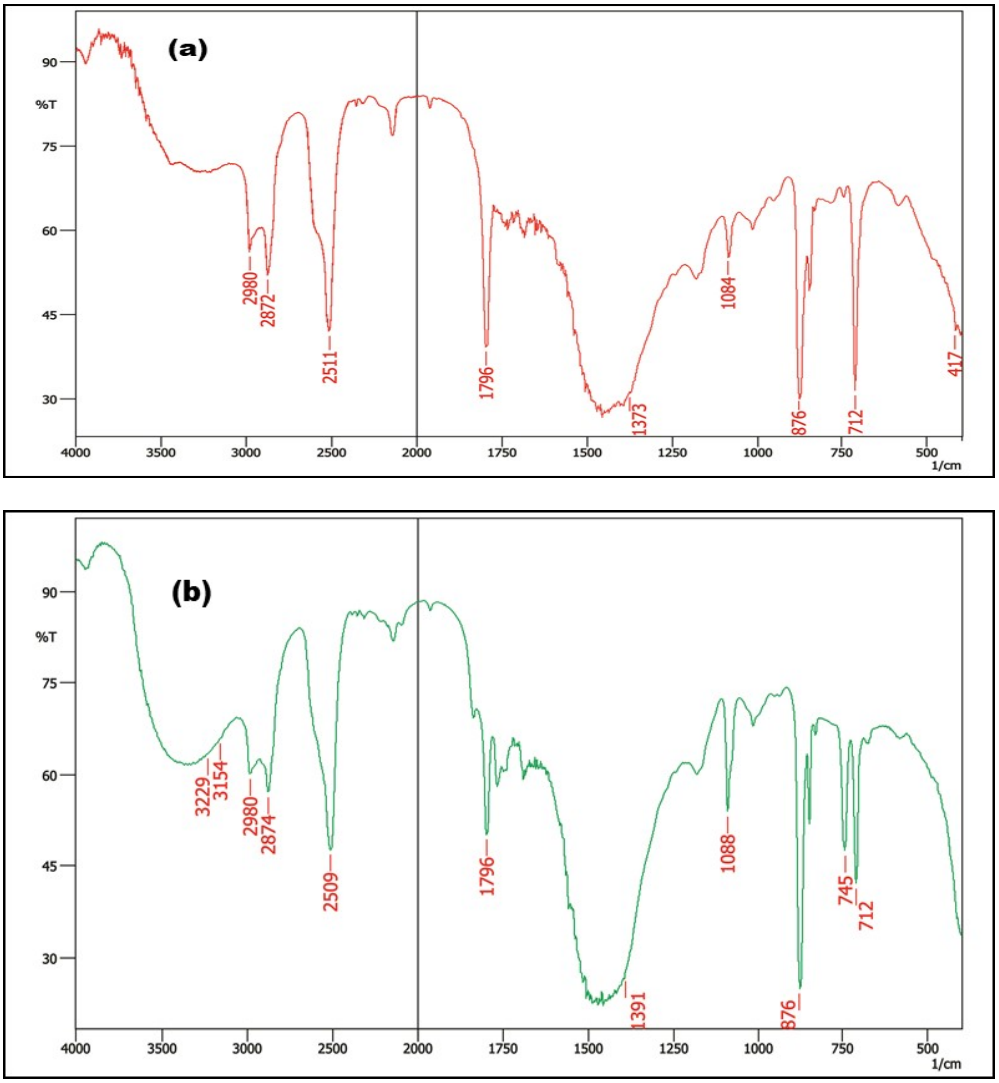

Fig.-9: FTIR of the Samples without (a), and with 20.00 ppm Malonic Acid (b)

Meanwhile, malonic acid contributes to the precipitation process as shown in Fig.-9b. The O-H stretching of the malonic acid is depicted in waves of 3154 and 3229 cm^{-1}, and again in the peak of 1391 cm^{-1}. Thus, it can be concluded that the malonic acid added has interacted with the $CaCO_3$ precipitation process. Firstly, the molecules may have attached to the surface of the nuclei preventing further nuclei growth, or attached to the surface of the crystals preventing further growth and causing surface imperfection (see Fig.-3b). Secondly, Ca^{2+} in the precipitating solution may have chelated with the carboxylic acid functional groups in the solution and hence reducing the supersaturation and subsequently decreasing the amounts of free Ca^{2+} available for nucleation and growth.[22]

TG-DTA Analysis

Thermal analysis was conducted via TG-DTA measurements and aimed at obtaining reaction peak temperature and types of reaction (endothermic or exothermic). Secondly, the analysis was also meant to observe the content of weakly bound water as well as the decomposition of calcium carbonate phases.

For TG-DTA measurements, approximately 20 mg of samples were weighed and then put into a platinum crucible and heated. Measurements were done simultaneously at a heating rate of 10 C min^{-1} under flowing air (500 cm^3/min). In all cases, the observed weight loss consisted of two steps (Figs.-10 and 11). The first step was between 4.00 to 6.00 wt% which occurred below 700ºC. The second step was between 700 and 850ºC, and it was ca. 43 - 50%.

For the samples formed without malonic acid after one minute of precipitation time (Fig.-10), the first loss of mass of 4.00 wt% was due to the release of weakly adsorbed (mobile) water. A subsequent loss of mass of 42.90 wt% was the result of $CaCO_3$ decomposition forming CaO and releasing CO_2. This is in a reasonably good agreement with the calculated value for the thermal decomposition of $CaCO_3$ to CaO which = 44%.

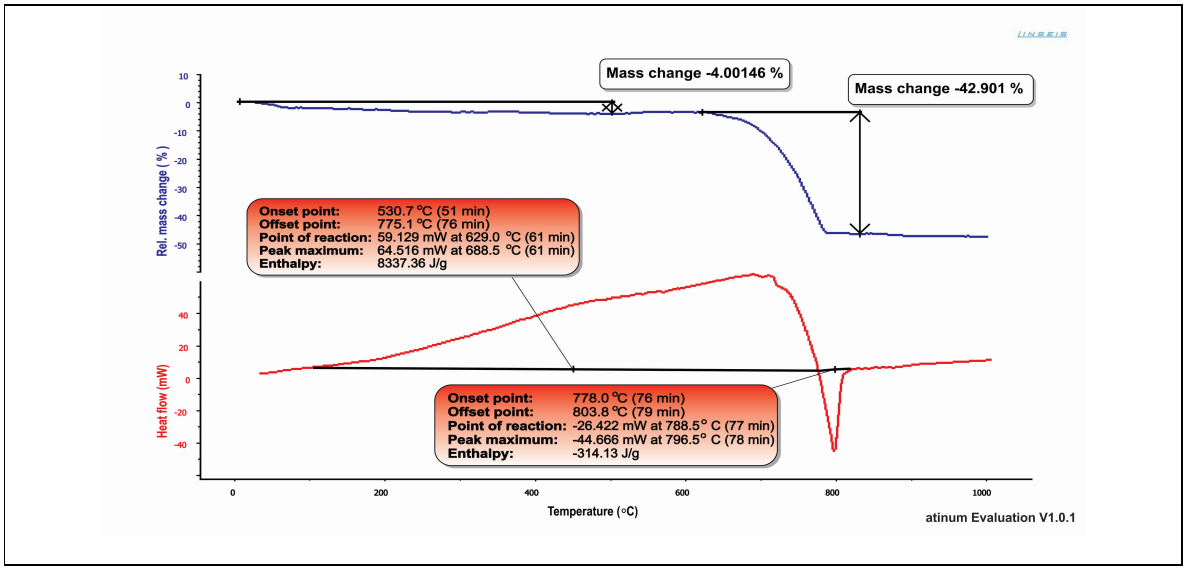

Fig.-10: TG-DTA Curves for One min precipitation in a Pure System (No Malonic Acid Addition)

A similar run but with the addition of 20.00 ppm malonic acid resulted in a higher weight loss for the two steps, namely 6.86 and 44.67 wt%, respectively (Fig.-11). These findings are similar to the results obtained by Li et al [26], on the decomposition kinetics of calcium carbonates containing carboxylic acids. It was postulated that the higher mass loss was due to the mass of the organic acids used.

At prolonged precipitation, i.e six hours and with the addition of 20.00 ppm malonic acid, a higher mass loss was observed for both steps: 5.10 and 49.08 wt %, respectively (Fig.-12). Again, these findings are similar to that of Li et al.[23] Longer precipitation time resulted in more malonic acid being adsorbed on the $CaCO_3$ precipitates, which was then released on heating.

DTA curve for one minute of precipitation time without malonic acid (see Fig.-9) shows endothermic peak which begins at 530.7ºC, reaches a peak at 688.5ºC, and terminates at 775.1ºC. It can be assumed that the endotherm was due to a change in the crystal structure and crystalline phase transition. The

subsequent exothermic characteristic begins at 778.0°C, reaches a peak at 796.5°C and ends at 803.8°C. This may represent the decomposition of calcite with the evolution of carbon dioxide.[24-26]

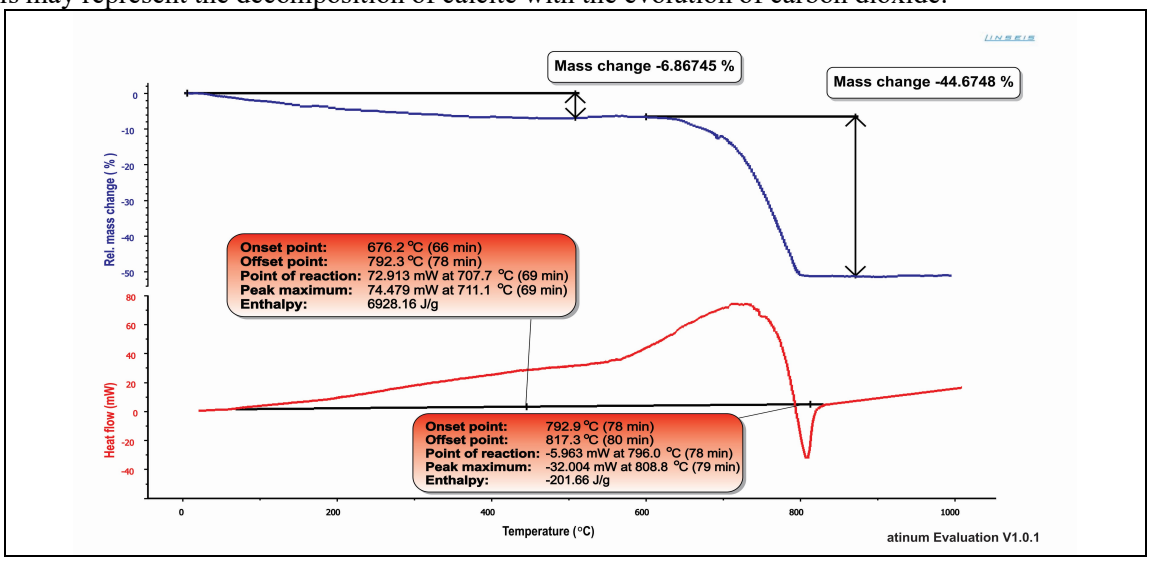

Fig.-11: TG-DTA Curves for one min precipitation with 20.00 ppm Malonic Acid

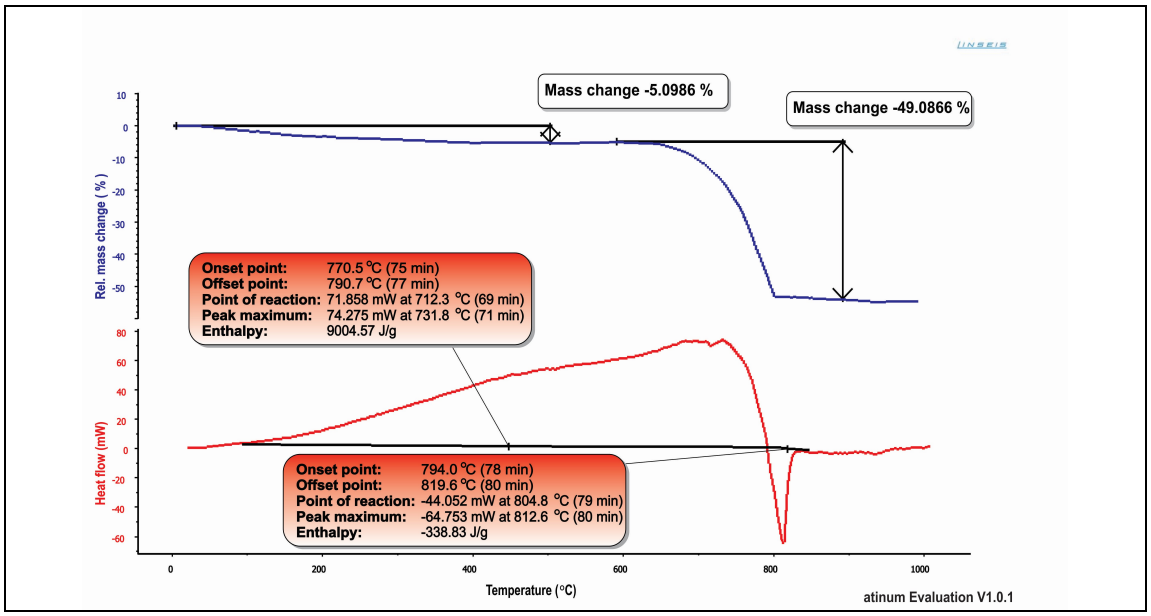

Fig.-12: TG-DTA Curves for Six Hours Precipitation with 20.00 ppm Malonic Acid

Similar TG patterns were observed for other cases (Figs.-10 and11), with higher weight loss for malonic acid addition. As for DTA measurements, higher onset point and reaction temperatures were recorded for malonic acid addition. The decomposition profiles of the precipitates in the pure system and the presence of malonic acid are similar (Figs.-10 to 12). The profiles, however, do not show accurately the phase transition of the $CaCO_3$ polymorph. These results are comparable to those of Li et al, on the decomposition of $CaCO_3$ precipitated with carboxylic acids.[23]

CONCLUSION

A laboratory batch-precipitation study to investigate the influence of malonic acid on $CaCO_3$ habit modification and polymorph changes was done by mixing stoichiometric amounts of $CaCl_2$ and Na_2CO_3 solutions. The effects were examined through SEM, XRD, FTIR and TG-DTA analysis, respectively.

For all experiments, the malonic acid in ppm amounts (0.00 and 20.00 ppm) was able to significantly influence both the morphology and the crystalline phases of $CaCO_3$. Hence it could be an effective modifier for $CaCO_3$.

Without malonic acid the three $CaCO_3$ phases grow at about the same rate as indicated by their similar precipitates amount. With the addition of malonic acid the number of calcite became dominant, while those of vaterite and aragonite decreased; indicating a greater inhibition of malonic acid towards vaterite and aragonite than that towards calcite. The difference in the inhibition can be the result of the variation in the surface characteristics. The surface of vaterite and aragonite is more irregular than that of calcite making it easier for additives to attach. However, at a higher malonic acid concentration (20.00 ppm), the growth of calcite is also inhibited as evident from the rounded edges of the calcite.

The longer the precipitation time, up to 48 h, the more pronounced the effect of malonic acid. The edges of calcite become rounded and causing irregular surfaces in certain spots. Also, vaterite and aragonite are still present indicating the stabilization effect of malonic acid towards the unstable phases of vaterite and aragonite.

TG-DTA analysis confirmed that longer precipitation time results in more malonic acid being adsorbed onto the surface of the $CaCO_3$ precipitates, which was subsequently released/liberated on heating. However, the TG-DTA analysis seems unsuitable to discriminate against the polymorph transition.

ACKNOWLEDGEMENT

The authors (SM, SS, ES) are grateful to the Ministry of Research, Technology and Higher Education of the Republic of Indonesia for funding the current work through the PDUPT grant: B.09/01.011/KP-PDUPT/III/2018

REFERENCES

1. S. Muryanto, and A. P. Bayuseno, *Powder Technology*, **253**, 602(2014), **DOI:**10.1016/j.powtec.2013.12.027
2. Z. Zou, W.J.E.M. Habraken, G. Matveeva, A.C.S.Jensen, L.Bertinetti, M.A.Hood, C-Y.Sun, P.U.P.A.Gilbert, I.Polishchuk, B.Pokroy, J.Mahamid, Y.Politi, S.Weiner, P.Werner, S.Bette, R.Dinnebier, U.Kolb, E.Zolotoyabko, P.Fratzl, *Science*, **363**, 396 (2019), **DOI:**10.1126/science.aav0210
3. M. Albéric, L. Bertinetti, Z. Zou, P.Fratzl, W.Habraken, Y.Politi, *Advanced Science*, **5(5)**, 1701000 (2018), **DOI:**10.1002/advs.201701000
4. H. Keller, J. Plank, *Cement and Concrete Research*, **54**, 1(2013), **DOI:**10.1016/j.cemconres.2013.06.017
5. L. Addadi, S. Raz, S. Weiner, *Advanced Materials*, **15(12)**, 959 (2003), **DOI:**10.1002/adma.200300381
6. D.Konopacka-Lyskawa, *Crystals*, **9**, 223(2019), **DOI:**10.3390/cryst9040223
7. K.-J.Westin and A.C.Rasmuson, *Journal of Colloid and Interface Science*, **282(2)**, 359(2005), **DOI:**10.1016/j.jcis.2004.09.071
8. M. M. Reddy, *Journal of Crystal Growth*, **352(1)**, 151(2012), **DOI:**10.1016/j.jcrysgro.2011.12.069
9. I.K.Al-Busaidi, R.S. Al-Maamari, M. Karimi, J. Naser, *Journal of Petroleum Science and Engineering*, **180**, 569 (2019), **DOI:**10.1016/j.petrol.2019.05.080
10. W.Mangestiyono, S.Muryanto, J.Jamari, A.P.Bayuseno, *Rasayan Journal of Chemistry* **12(1)**, 192 (2019), **DOI:**10.31788/RJC.2019.1215055
11. T. Rabizadeh, C. L. Peacock, and L. G. Benning, *Mineralogical Magazine*, **78(6)**, 1465 (2014), **DOI:**10.1180/minmag.2014.078.6.13
12. N.Karaman, W.Mangestiyono, S.Muryanto, J.Jamari, A.P.Bayuseno, *Rasayan Journal of Chemistry*, **12(04)**, 1734 (2019), **DOI:**10.31788/RJC.2019.1245380
13. D. Aquilano, M. Bruno, and L. Pastero, *Crystal Growth and Design*, **20(4)**, 2497(2020), **DOI:** 10.1021/acs.cgd.9b01651
14. U. Aschauer, J. Ebert, A. Aimable, and P. Bowen, *Crystal Growth and Design*, **10(9)**, 3956 (2010), **DOI:**10.1021/cg1005105

15. E. P. Peters, G. J. Schlakman, and E. N. Yang, Senior Design Reports (CBE).107 (2018)
16. B. Leng, F. Jiang, K. Lu, W.Ming, Z.Shao, *Crystal Engineering. Communications*, **12**, 730 (2010), **DOI:**10.1039/B909413J
17. M. Ø. Olderøy, M. Xie, B. L. Strand, K. I. Draget, P. Sikorski, and J.-P. Andreassen, *Crystal Growth and Design*, **11(2)**, 520(2011), **DOI:**10.1021/cg101337g
18. C. Jimenez-Lopez, A. B. Rodriguez-Navarro, J. M. Domínguez-Vera, J. M. Garcia-Ruiz, *Geochimica et Cosmochimica Acta*, **67(9)**, 1667(2003), **DOI:**10.1016/S0016-7037(02)01275-9
19. M. R. Derrick, D. Stulik, J. M. Landry, Infrared Spectroscopy in Conservation Science, Getty Conservation Institute, Los Angeles, 95 (1999)
20. M. Sadeghi, M. H. Husseini, *Journal of Applied Chemistry Research*, **7**, 39 (2013)
21. V. J. Bruckman, and K. Wriessnig, *Environmental Chemistry Letters*, **11**, 65(2013), **DOI:**10.1007/s10311-012-0380-4cccc
22. D. J. Tobler, J.D.Rodriguez-Blanco, K.Dideriksen, N.Bovet, K.K.Sand, S.L.S.Stipp, *Advanced Functional Materials*, **25**, 3081 (2015), **DOI:**10.1002/adfm.201500400
23. X-G. Li, Y.Lv, B-G. Ma, W-Q.Wang, S-W.Jian, *Arabian Journal of Chemistry* (2013), **DOI:** 10.1016/j.arabjc.2013.09.026
24. L. Fedunik-Hofman, A. Bayon, S. W. Donne, *Applied Science*, **9**, 460 (2019), **DOI:**10.3390/app9214601
25. S. Gunasekaran, G. Anbalagan, *Bulletin of Materials Science*, **30(4)**, 339(2007), **DOI:**10.1007/s12034-007-0056-z
26. Firnanelty, S.Sugiarti and Charlena, *Rasayan Journal of Chemistry*, **10(2)**, 570(2017), **DOI:**10.7324/RJC.2017.1021465

[RJC-5804/2020]